Neurogastroenterology & Motility

Neurogastroenterol Motil (2014) doi: 10.1111/nmo.12371

Distinct subcellular localization of the neuronal marker HuC/D reveals hypoxia-induced damage in enteric neurons

A.-S. DESMET, C. CIRILLO & P. VANDEN BERGHE

Laboratory for Enteric NeuroScience (LENS), Translational Research Center for GastroIntestinal Disorders (TARGID), University of Leuven, Leuven, Belgium

Key Messages

- We investigated the subcellular localization of pan-neuronal marker HuC/D in mouse myenteric neurons in different conditions.
- Immunohistochemical techniques were used to label HuC/D and glial fibrillary acidic protein (GFAP) expression in the myenteric plexus of the mouse colon.
- Hypoxia-induced damage results in a predominantly nuclear localization of HuC/D.
- Nuclear HuC/D localization was associated with the activation of a non-apoptotic genetic program and distortion of the glial network.
- HuC/D protein is more than a pan-neuronal marker as its subcellular localization reflects the health status of the neurons.

Abstract

Background *Correct neuronal identification is essential to study neurons in health and disease. Although commonly used as pan-neuronal marker, HuC/D's expression pattern varies substantially between healthy and (patho)physiological conditions. This heterogenic labeling has received very little attention. We sought to investigate the subcellular HuC/D localization in enteric neurons in different conditions.* ***Methods*** *The localization of neuronal RNA-binding proteins HuC/D was investigated by immunohistochemistry in the mouse myenteric plexus using different toxins and caustic agents. Preparations were also stained with Sox10 and glial fibrillary acidic protein (GFAP) antibodies to assess enteric glial cell appearance.* ***Key Results*** *Mechanically induced tissue damage, interference with the respiratory chain and oxygen (O_2) deprivation increased nuclear HuC/D immunoreactivity. This effect was paralleled by a distortion of the GFAP-labeled glial network along with a loss of Sox10 expression and coincided with the activation of a non-apoptotic genetic program. Chemically induced damage and specific noxious stimuli did not induce a change in HuC/D immunoreactivity, supporting the specific nature of the nuclear HuC/D localization.* ***Conclusions & Inferences*** *HuC/D is not merely a pan-neuronal marker but its subcellular localization also reflects the condition of a neuron at the time of fixation. The functional meaning of this change in HuC/D localization is not entirely clear, but disturbance in O_2 supply in combination with the support of enteric glial cells seems to play a crucial role. The molecular consequence of changes in HuC/D expression needs to be further investigated.*

Keywords *enteric neurons, GFAP, glial cells, HuC/D, hypoxia.*

Address for Correspondence
Pieter Vanden Berghe, Laboratory for Enteric NeuroScience (LENS), TARGID, University of Leuven, Herestraat 49, ON1, mailstop 701, Leuven B-3000, Belgium.
Tel: +32 16 33 01 53; fax: +32 16 34 59 39;
e-mail: pieter.vandenberghe@med.kuleuven.be
Received: 31 January 2014
Accepted for publication: 29 April 2014

INTRODUCTION

Correct identification of neurons is critical to investigate and understand morphological and functional changes that may occur during health and disease. HuC/D protein is routinely used as neuronal marker both in the central and in the peripheral nervous system. HuC/D is not only neuron-specific, but it also labels all neurons rather than specific subpopulations; hence the adjective 'pan-neuronal' marker.[1–3] Another practical advantage of the HuC/D staining is that quantification of individual neurons is made easy, as unlike other commonly used neuronal markers (PGP 9.5, peripherin and neurofilament), it does not label neuronal processes.[1] HuC/D belongs to the family of Hu proteins, the human homologs of Drosophila Melanogaster Embryonic Lethal Abnormal Vision (ELAV) proteins.[4] Hu proteins were first discovered as autoantibodies in the circulation of patients with paraneoplastic encephalomyelitis (Hu syndrome), who aside from their neuro-immune problems also suffer from gastrointestinal problems.[5–7] Functionally, HuC/D, and Hu proteins in general, regulates the stability of specific mRNA and thereby modulate and control the precise temporal expression of certain proteins.[8,9] Moreover, Hu proteins also regulate mRNA localization and microRNA-mediated repression.[10] Hu proteins can bind specific mRNA (e.g., VEGF, AChE, BDNF, GAP43)[11–16] through particular recognition motifs that interact with adenine uridine-rich elements in the 3′ untranslated region. Because of this role in mRNA stabilization, HuC/D normally resides in the cytosol, but it can also be present in the nucleus where specific transporter proteins that shuttle Hu proteins through the nuclear envelope have been described.[17] Although its role in the nucleus is still elusive, HuC/D has been suggested to be involved in regulation of polyadenylation and alternative splicing.[10]

The heterogeneity with respect to expression levels in different subcellular compartments, which is apparent in many published micrographs[10,18–20] is not restricted to the enteric nervous system (ENS), but is also present in the central nervous system. Strangely, this heterogeneity has been largely ignored, except for some intestinal ischemia-reperfusion studies, where nuclear expression of Hu proteins, associated with elevated nitrosylation levels,[21,22] was reported. The underlying reasons for this change in subcellular localization are still unknown, but the HuC/D expression pattern may reflect a condition of neuronal stress and damage, during which altered regulation of mRNA or alternative splicing is needed. A dedicated study of HuC/D expression patterns is thus warranted to understand what extra information HuC/D labeling might yield about neuronal health.

Therefore, the aim of this study was to gain insight in the mechanisms underlying different HuC/D expression patterns in ENS neurons. We used myenteric plexus preparations from mouse colon and mimicked neuronal damage *in vitro*. As it is well established that enteric neurons are tightly packed and interact with glial cells within the ENS, we also evaluated the expression of typical glial markers to investigate whether glial abnormalities would parallel or correspond to the altered HuC/D expression.

We found that oxygen (O_2) deprivation is an important trigger to alter intracellular localization of HuC/D in enteric neurons. Under low oxygen conditions, an increased nuclear HuC/D immunoreactivity was found, a phenomenon that was associated with severe abnormalities in the enteric glial network.

MATERIALS AND METHODS

Animals and tissue preparation

C57BL/6 mice with *ad libitum* access to standard chow (Sniff; Soest, Germany) and tap water were used in this study. They were sacrificed by cervical dislocation as approved by the animal Ethics Committee of the University of Leuven, Belgium.

The colon was removed and put in Krebs solution (120.9 mM NaCl [Normapur VWR, Singapore, Singapore], 5.9 mM KCl [Normapur VWR], 1.2 mM $MgCl_2$ [Normapur VWR], 11.5 mM glucose [Merck, Darmstadt, Germany], 14.4 mM $NaHCO_3$ [Merck], 1.2 mM NaH_2PO_4, and 2.5 mM $CaCl_2$ [Merck]) oxygenated with 95% O_2/5% carbon dioxide (CO_2). The mid and distal colon was cleared from fat, cut along the mesenteric border and pinned flat in a Sylgard Petri dish. The mucosa and submucosal layers and longitudinal muscle layers were then removed to obtain myenteric plexus preparations. Tissue incubations were performed in small glass dishes (diameter: 3 cm) containing a Sylgard layer. The dissected myenteric plexus was pinned and lifted from the bottom to allow sufficient circulation of nutrients, buffer, and O_2 in the entire dish.

Different experimental conditions were designed to induce changes in subcellular HuC/D localization. We applied (i) mechanically induced tissue damage, (ii) chemically induced tissue damage, (iii) endoplasmic-reticulum (ER) stress-induced damage, (iv) pro-inflammatory cytokines-induced damage, (v) specific inhibition of the respiratory chain, (vi) O_2 deprivation, and (vii) toxin-induced glial damage (see Table 1).

In a first set of experiments, the myenteric plexus was kept in oxygenated Krebs solution at room temperature (RT) 1, 2, or 4 h before fixation to test whether dissection-induced tissue damage would cause changes in HuC/D localization. Mechanical damage was induced by gently scratching (±0.5 mm) the tissue using a blunt surgical blade in the middle of a 1 cm^2 myenteric plexus preparation (Table 1). Chemical damage was induced by incubating the myenteric plexus in Krebs solution containing 0.1% Benzalkoniumchloride (BACl, 1 h). O_2 deprivation, to mimic ischemic conditions, was induced by continuous bubbling with 100% N_2 (1–2 h: pH 9), while pH effects were tested in Krebs (pH:

Table 1 Specification of different incubation conditions

Experiment	Treatment	Incubation conditions
Mild damage	Time (after dissection)	Krebs buffer (RT, 1–4 h)
Mechanical damage	Nerve crushing using blunt surgical blade	Krebs buffer (RT, up to 2 h)
Chemically induced damage	0.1% Benzalkoniumchloride (BACl)	Krebs buffer (RT, up to 2 h)
Oxygen deprivation (hypoxia)	Bubbled with 100% N_2	Krebs buffer (RT, up to 2 h)
pH effect	pH 6.45 bubbled with 100% O_2 pH 8.1 bubbled with 100% O_2	Krebs buffer (RT, up to 2 h)
Triton X-100	5% Triton X-100	
ER stress-induced damage	100 nM thapsigargin	Complete medium (37 °C, 3–24 h)
Pro-inflammatory cytokines	10 ng/mL TNF-α + 10 ng/mL IL-1β	Complete medium (37 °C, 3–24 h)
Mitochondrial complex I inhibition	100 nM rotenone	Complete medium (37 °C, 3–24 h)
Toxin-induced glial damage	10 μM fluorocitrate	Complete medium (37 °C, 3–24 h)

Table 2 Specification of antibodies, with dilution, host, and source

Antigen	Host	Dilution	Source
HuC/D	Mouse	1/500	Invitrogen Life Technologies, Ghent, Belgium
GFAP	Chicken	1/5000	Abcam, Cambridge, UK
Sox10	Goat	1/300	Santa Cruz Biotechnologies, Santa Cruz, CA, USA
c-Fos	Rabbit	1/500	Santa Cruz Biotechnologies
Hu	Human	1/5000	Lennon[7]
Mouse-IgG Alexa 488	Donkey	1/1000	Molecular Probes, Leiden, The Netherlands
Mouse-IgG Alexa 594	Donkey	1/1000	Molecular Probes
Chicken-IgG Alexa 594	Goat	1/1000	Molecular Probes
Goat-IgG Alexa 594	Donkey	1/1000	Molecular Probes
Rabbit-IgG Alexa 594	Donkey	1/1000	Molecular Probes
Human-IgG FITC	Goat	1/250	Jackson Immuno Labs, West grove, PA, USA

6.45–8.1) bubbled with O_2 instead of carbogen gas (1–2 h of incubation; Table 1). In a last set of experiments, tissues were incubated for 2 h in Krebs buffer containing high concentrations (5%) of Triton X-100 (Table 1).

For longer incubations we used a complete medium DMEM/F12 1:1 (Gibco®; Invitrogen, Merelbeke, Belgium) enriched with 2 mM L-glutamine + 50 U/mL Penicillin + 50 U/mL Streptomycin + 10% fetal bovine serum (all from Lonza, Group Ltd, Basel, Switzerland) and placed the myenteric plexus in an incubator at 37 °C (5% CO_2/95% air). ER stress was induced by thapsigargin (100 nM), while an inflammatory condition was modeled by adding a mixture of 10 ng/mL tumor necrosis factor-alpha (TNF-α) + 10 ng/mL interleukin-1beta (IL-1β) to the culture medium (Table 1). Rotenone (100 nM) was used to specifically interfere with the electron transport chain in mitochondria (Table 1). Glial damage was induced by incubating the plexus in complete medium containing 10 μM fluorocitrate (Table 1).

At the end of each experimental condition, tissues were fixed for 45 min at RT in 4% paraformaldehyde (Sigma-Aldrich, Bornem, Belgium) diluted in 0.2 M PBS (29.6 mM NaH_2PO_4 [Merck], 184.7 mM Na_2HPO_4 [Normapur VWR], pH 8) and then thoroughly washed in 0.1 M PBS (1.54 mM KH_2PO_4 [Merck], 155.17 mM NaCl [Normapur VWR], 2.71 mM Na_2HPO_4 [Normapur VWR]).

Immunohistochemistry

Tissues were incubated for 2 h (overnight for c-Fos immunostaining) at RT in blocking solution containing 0.5% Triton X-100 diluted in 0.1 M PBS and 4% serum of the secondary antibody hosts followed by incubation overnight at 4 °C with the primary antibodies diluted in blocking medium (Table 2). After washing in PBS, the tissues were incubated for 2 h at RT with appropriate secondary antibodies (Table 2) diluted in blocking buffer. After washing in PBS, tissues were mounted on a microscope slide in citifluor (Citifluor Ltd., Leicester, UK). To assure that the nuclear envelope was sufficiently permeable, we also performed an immunohistochemical labeling in solutions containing 5% Triton X-100 instead of 0.5%.

The Invitrogen antibody was used for all HuC/D stainings, which were double-checked for specificity in a select set of experiments (data not shown), using a human anti-Hu antibody (Source: Lennon[7]).

TUNEL assay

After immunohistochemistry, a TUNEL assay was performed using an *in situ* cell death detection kit (Roche Applied Science, Vilvoorde, Belgium). After washing in PBS, tissues were incubated for 2 min on ice in permeabilization solution containing 0.1% Triton X-100 and 0.1% sodium citrate. The samples were then washed in PBS and the TUNEL reaction mixture was added to the samples for 1 h at 37 °C in humid environment. Afterward, the tissues were washed in 0.1 M PBS and mounted on a microscope slide.

Drugs and materials

Rotenone, thapsigargin, IL-1β, and fluorocitrate were from Sigma-Aldrich, while TNF-α was from Invitrogen. Benzalkoniumchloride was kindly provided by Prof. Herman Van Pee (Faculty of Pharmaceutical Sciences, University of Leuven).

Data presentation and statistical analysis

Immunohistochemical stainings were visualized under an epifluorescence microscope (BX41 Olympus, Aartselaar, Belgium) with specific filter cubes (Ex/DM/Em in nm: 325–375/400/435–485; 460–495/505/510–550; 570–590/595/600–660) for respectively blue, green, and red probes. An XM10 (Olympus) camera using Cell^F software was used to record the images. Before overlay, pictures were adjusted for contrast and brightness. Three ganglia per tissue were analyzed for each experimental condition in five independent experiments. Exposure times were kept constant to assure a correct comparison between different experiments. The intensity of HuC/D staining was then calculated in the nucleus and cytosol of each neuron (Cell^F software) to calculate the expression ratio, which will be referred to as the HuC/D intensity ratio throughout the manuscript. The statistical analysis was performed with Graphpad prism software. As data were not normally distributed (D'Agostino & Pearson omnibus normality test), non-parametric Mann–Whitney U and Kruskal–Wallis followed by Dunns *post hoc* tests were used to compare different conditions. The data are presented by mean ± SEM. Differences were considered to be significant if the p value was smaller than 0.05.

RESULTS

HuC/D labeling shows substantial heterogeneity in its subcellular localization

Immunohistochemical labeling reveals that HuC/D can be expressed at different levels in the cytosol and in the nucleus of neurons (Fig. 1A). In a first set of experiments, during which tissues were kept in oxygenated Krebs buffer at RT before fixation, we found that the presence of HuC/D in the nucleus increased as incubation time progressed (time 0: 5.4 ± 1.01 *vs* 2 h: 21.4 ± 3.4%; $^{**}p < 0.01$, 1 h: 9.5 ± 2.3% *vs* 4 h: 39.6 ± 3.6%; $^{***}p < 0.001$, time 0 *vs* 4 h; $^{***}p < 0.001$; Fig. 1C, left). In addition, we found that the number of neurons per ganglion was not significantly different after different periods of incubation (Fig. 1C, right). In addition, we found that this was associated with alterations of the

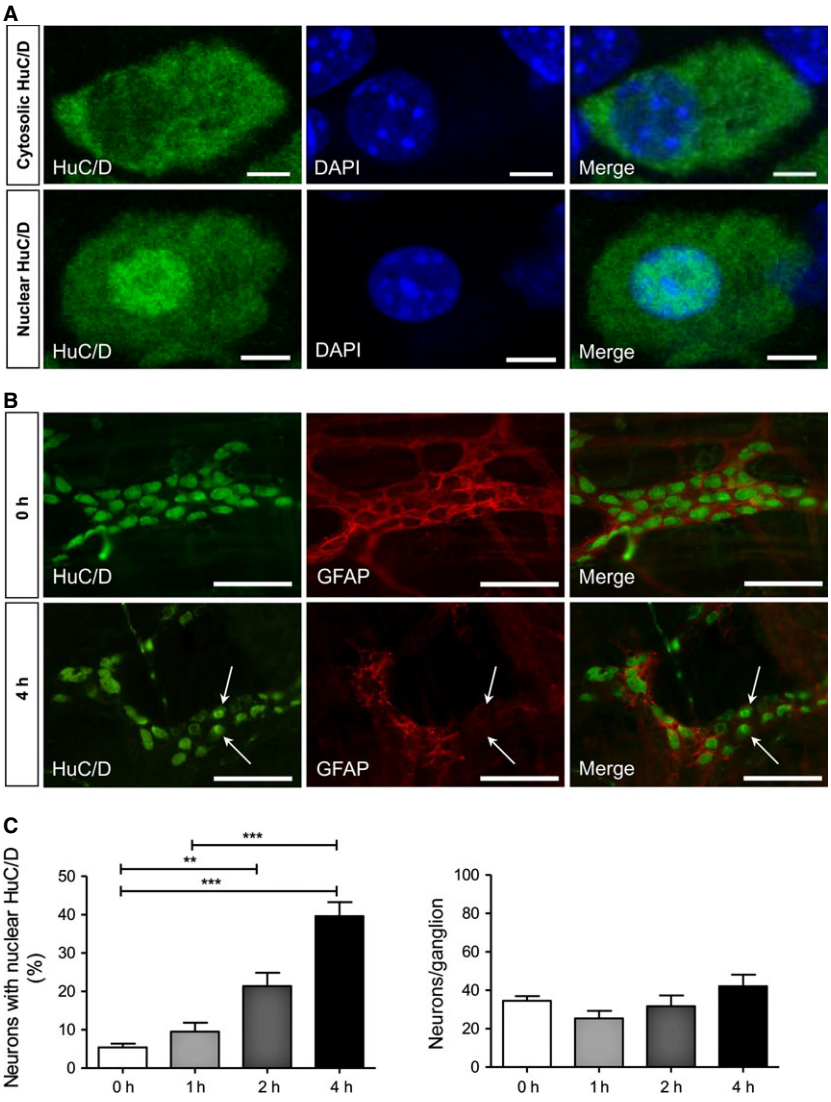

Figure 1 Heterogeneous expression and localization of the neuronal marker HuC/D in myenteric neurons. (A, *top left*) Confocal images of a neuron stained with an antibody against HuC/D: note the fairly homogeneous staining in the cytosol, counterstained with DAPI (A, *top middle*), and merged image (A, *top right*). (A, *bottom left*) Confocal images of a neuron stained with an antibody against HuC/D, DAPI counterstaining (A, *bottom middle*), and merged image (A, *bottom right*). Note the brighter staining in the nucleus; scale bars: 5 μm. (B) Representative immunohistochemical staining (HuC/D and glial marker GFAP) of a tissue that was fixed immediately (time 0, *top*) or 4 h (*bottom*) after dissection. Note the intense nuclear HuC/D staining (arrows, *left*) and disrupted GFAP staining (arrows, *middle*). Merged image in B, *right*; scale bars: 100 μm. (C) Graphs showing the number of neurons with nuclear HuC/D compared to the total number of neurons (in %, per ganglion) in tissues fixed at different time points after dissection ($^{**}p < 0.01$, $^{***}p < 0.001$; *left*) and the total number of neurons/ganglion ($p > 0.05$; *right*).

enteric glial network as shown by a loss and distortion of GFAP expression (Fig. 1B). We hypothesize that the tissue damage induced by dissection progressively affects neurons and enteric glial cells during RT incubation. To further characterize the nature of the specific subcellular HuC/D localization, we performed different sets of *in vitro* experiments ranging from mechanical damage and toxin exposure to significant pH changes and O_2 deprivation.

Mechanical damage induces changes in HuC/D expression in myenteric neurons

To test whether mechanical damage (to mimic nerve crushing) could affect the intracellular localization of the HuC/D protein, we made a scratch using a blunt surgical blade in the middle of a square cm myenteric plexus preparation (Fig. 2A). After 2 h at RT, we found that the HuC/D staining was more prominent in the nucleus compared to the control condition (HuC/D intensity ratio: 2.0 ± 0.14 *vs* 1.2 ± 0.06; $^{***}p < 0.001$; Fig. 2C, left). Interestingly, this increase was only found in the damaged region (2.0 ± 0.14 *vs* 0.9 ± 0.03; $^{***}p < 0.001$; Fig. 2C, left), indicating that the damage did not progressively affect other areas. Here, enteric glial network distortion and fragmented GFAP pattern were also visible in close proximity to the mechanical damage (Fig. 2A).

BACl does not affect HuC/D expression in myenteric neurons

We sought to produce damage over a larger area by incubating the tissue in the presence of BACl, a cationic surfactant used to damage and kill myenteric neurons.[2,3–2,5] We found no additive effect of 0.1% BACl (1 h) on the HuC/D intensity ratio compared to control (1.6 ± 0.06 *vs* 1.5 ± 0.08; $p > 0.05$; Fig. 2C, right). The enteric glial network was weakly affected but only in specific regions (Fig. 2B).

Effect of pathological and noxious stimuli on HuC/D expression in myenteric neurons

As the nuclear HuC/D expression was more intense when cellular damage was elicited *in vitro*, we also tested whether other noxious stimuli, as used in disease models, had similar effects. During tissue incubation, the number of HuC/D positive neurons remained constant and comparable to directly fixed

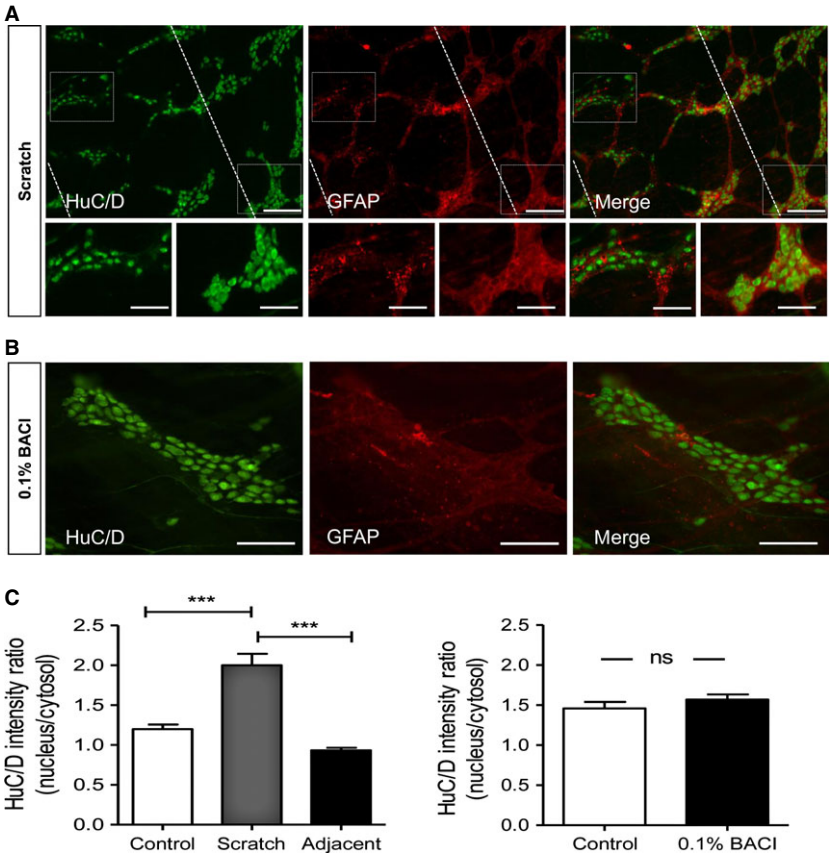

Figure 2 Mechanical damage causes changes in HuC/D expression in myenteric neurons. (A) Representative immunostaining of the myenteric plexus in a tissue that was gently scratched (in between the dashed lines). *Left*: HuC/D expression is more intense in the nucleus at the location of the scratch (enlarged picture, *left insets*) compared to regions adjacent to the scratch (enlarged picture, *right insets*). *Middle*: Changes in HuC/D staining were associated with distorted GFAP expression. Merged images in A, *right*. (A, *bottom row*) Enlarged images of the scratch (*left*) and adjacent to scratch (*right*); scale bars: 200 μm in the top, 100 μm in the bottom row. (B) Representative immunostaining of a myenteric ganglion exposed to 0.1% BACl. *Left*: HuC/D expression is homogeneous in the neuronal cell body. *Middle*: BACl caused distortion of GFAP expression. Merged image in B, *right*; scale bars: 100 μm. (C) Graphs showing the mean HuC/D intensity ratio between nucleus/cytosol after mechanical damage (*left*; $^{***}p < 0.001$) and after application of cationic surfactant BACl (*right*; $p > 0.05$).

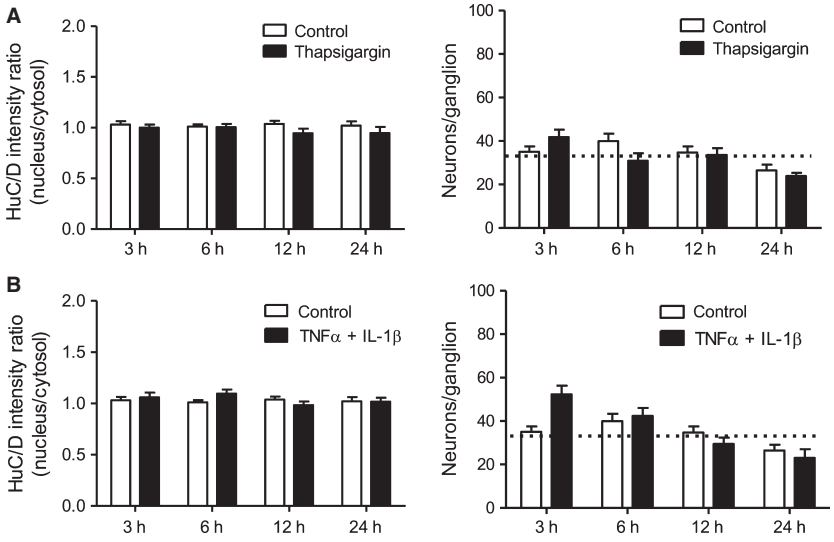

Figure 3 Effect of ER stress and pro-inflammatory cytokines on HuC/D expression in myenteric neurons. (A) Graphs showing the mean HuC/D intensity ratio nucleus/cytosol (no significant differences were found; $p > 0.05$; *left*) and the total number of HuC/D-positive neurons/ganglion (*right*) after incubation with the ER stress inducer, thapsigargin, at different time points. (B) Graphs showing the mean HuC/D intensity ratio nucleus/cytosol (no significant differences were found; $p > 0.05$; *left*) and the total number of HuC/D-positive neurons/ganglion (*right*) after incubation with a mixture of pro-inflammatory cytokines, TNFα + IL-1β, at different time points. The dashed line in (A) and (B) represents the average number of HuC/D-positive neurons per ganglion in tissues that were immediately fixed (34.5 ± 2.4).

tissue (dashed line Fig. 3, right), with the sole exception of a small reduction at 24 h.

Thapsigargin-induced ER stress. Thapsigargin is known to act as an ER stressor as it inhibits the SERCA pump, resulting in Ca^{2+} depletion of the ER.[26,27] We used thapsigargin (100 nM) to investigate whether ER stress, and the consecutive unfolded protein response pathway, would induce changes in HuC/D expression, but we found no differences in the HuC/D intensity ratio between control and treated condition (all $p > 0.05$; Fig. 3A, left).

Pro-inflammatory mediators (TNF-α + IL-1β). As inflammation plays a crucial role in many gastrointestinal disorders, myenteric plexus preparations were exposed to a mixture of pro-inflammatory cytokines TNF-α and IL-1β.[28] Again, no significant differences were found in the HuC/D intensity ratio between control and treated condition (all $p > 0.05$; Fig. 3B, left).

Blockade of the respiratory chain results in HuC/D expression changes

We used the environmental toxin rotenone, a well-known blocker of mitochondrial complex 1[29,30] to interfere with the respiratory chain. The HuC/D intensity ratio was significantly higher in treated (3–6 h) compared to control conditions (ctrl 3 h: 1.03 ± 0.03 *vs* rotenone 3 h: 1.17 ± 0.06; $^{*}p < 0.05$, ctrl 6 h: 1.01 ± 0.02 *vs* rotenone 6 h: 1.27 ± 0.03; $^{**}p < 0.01$), while this increase vanished after longer incubation (Fig. 4B, left). We also found that the number of HuC/D-positive neurons per ganglion decreased the longer the tissue was incubated (ctrl 6 h: 39.96 ± 3.4 *vs* ctrl 24 h: 26.43 ± 2.7; $^{*}p < 0.05$, rotenone 3 h: 46.25 ± 4.0 *vs* rotenone 24 h: 21.67 ± 3.2; $^{***}p < 0.001$, rotenone 6 h: 47.50 ± 4.5 *vs* rotenone 24 h; $^{***}p < 0.001$; Fig. 4B, right; direct: 34.5 ± 2.4 *vs* control 24 h: 26.43 ± 2.7; $^{*}p < 0.05$, direct *vs* rotenone 24 h: 21.67 ± 3.2; $^{**}p < 0.01$; Fig. 4B, right). Similar to other conditions, we also found the GFAP expression pattern distorted after rotenone application (Fig. 4A).

Hypoxia but not pH induces an increase in nuclear HuC/D immunoreactivity

During the experiments in which tissues were mechanically damaged, the question arose as to whether it was shortage of O_2 that could be responsible for the change in HuC/D localization. We tested the effect of hypoxia by bubbling with N_2 to deplete O_2 (Fig. 5A).[31,32] We found that the HuC/D intensity ratio was significantly increased compared to control both after 1 h (1.0 ± 0.03 *vs* 1.4 ± 0.07; $^{***}p < 0.001$) and 2 h (1.4 ± 0.07 *vs* 1.8 ± 0.08; $^{***}p < 0.001$) incubation at RT (Fig. 5B, left). In the vicinity of neurons with predominant nuclear HuC/D expression, the GFAP pattern was also fragmented and completely different from a normal GFAP expression pattern (Fig. 5A).

To exclude that the increased HuC/D intensity ratio under hypoxic conditions was due to pH changes, we incubated tissues at different pH. We found that neither an increase (pH 8.1) nor a decrease (pH 6.4) in pH had an effect on the HuC/D intensity ratio (ctrl 2 h: 1.2 ± 0.06 *vs* pH 6: 1.1 ± 0.1 *vs* pH 8: 1.0 ± 0.1; $p > 0.05$; data not shown).

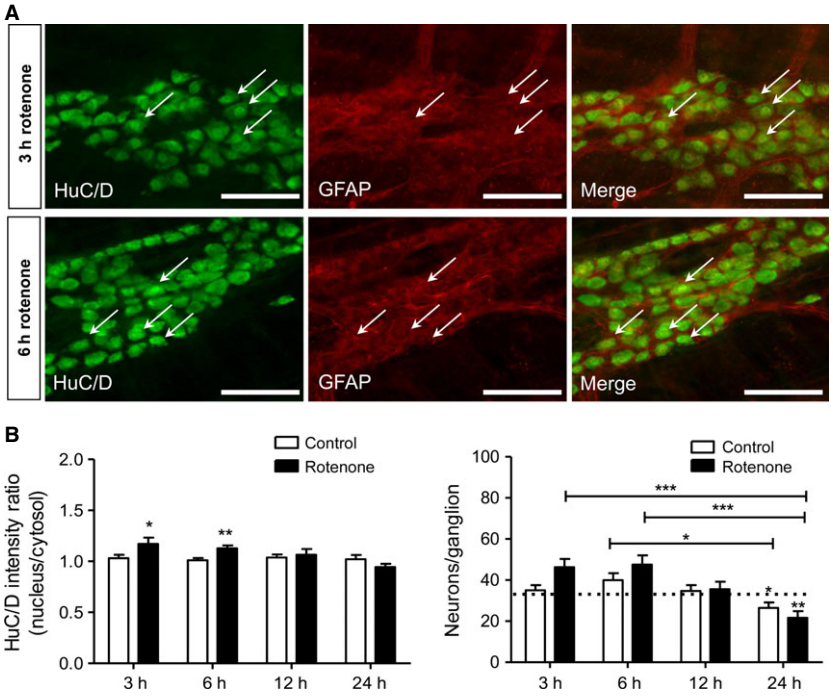

Figure 4 Inhibition of the respiratory chain changes the HuC/D expression in myenteric neurons. (A) Representative immunohistochemical staining of the neuronal marker HuC/D (*left*) and glial marker GFAP (*middle*) after 3 h (*top*) and 6 h (*bottom*) rotenone (100 nM) incubation. Note the intense nuclear HuC/D staining (arrows, *left*) and the distortion of GFAP staining (arrows, *middle*). Merged images in A, *right*; scale bars: 100 μm. (B) Graphs showing the effect of rotenone after 3 and 6 h incubation on the mean HuC/D intensity ratio nucleus/cytosol (*left*; $^{*}p < 0.05$, $^{**}p < 0.01$ *vs* ctrl) and the number of HuC/D-positive neurons/ganglion (*right*; ctrl 24 h *vs* direct; $^{*}p < 0.05$, rotenone 24 h *vs* direct; $^{**}p < 0.01$ and effect over time $^{*}p < 0.05$, $^{***}p < 0.001$). The dashed line shows the average number of neurons per ganglion in a directly fixed tissue (34.5 ± 2.4).

Enteric glial network distortion parallels nuclear HuC/D expression in neurons

As glial cells in the gut are known to play an important supportive role for neurons in the ENS,[33,34] we analyzed the enteric glial network using GFAP staining after each experimental condition. We found that when HuC/D expression was predominant in the nucleus, there was a parallel distortion of the GFAP pattern. In addition, Sox10 immunoreactivity was not detectable in the vicinity of myenteric neurons with high HuC/D intensity ratios (Fig. 6A),

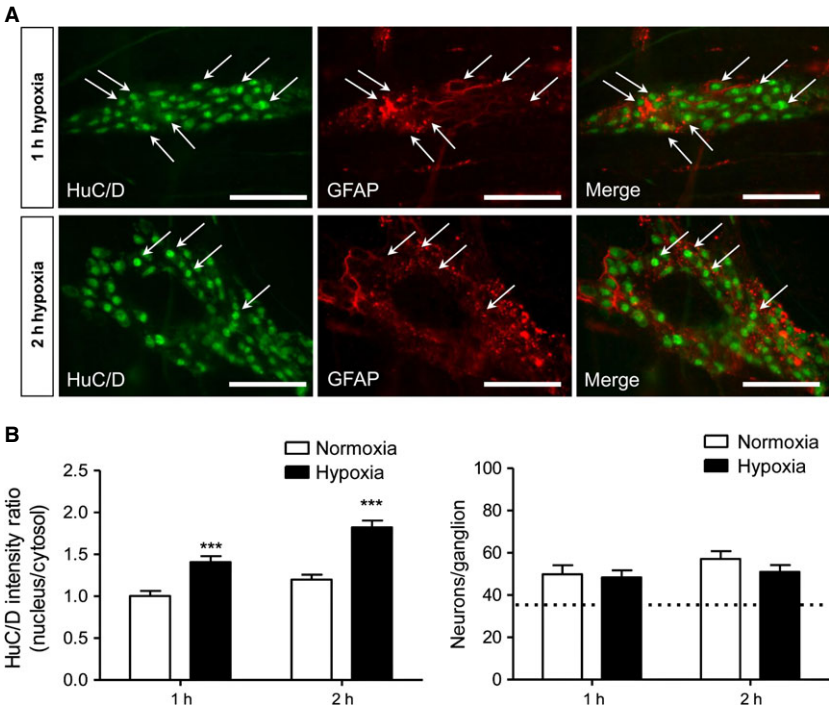

Figure 5 Hypoxia but not altered pH changes in HuC/D expression in myenteric neurons. (A) Representative immunohistochemical staining of HuC/D (*left*) and GFAP (*middle*) in a myenteric ganglion after incubation in hypoxic conditions (1 h *up*, 2 h *bottom*). Note the intense nuclear HuC/D staining (arrows, *left*) and the distorted GFAP staining (arrows, *middle*). Merged images in A, *right*; scale bars: 100 μm. (B) Graphs showing the effect of hypoxia (1 and 2 h) on the mean HuC/D intensity ratio nucleus/cytosol ($^{***}p < 0.001$ *vs* normoxia (*left*) and the total number of HuC/D-positive neurons/ganglion (*right*)).

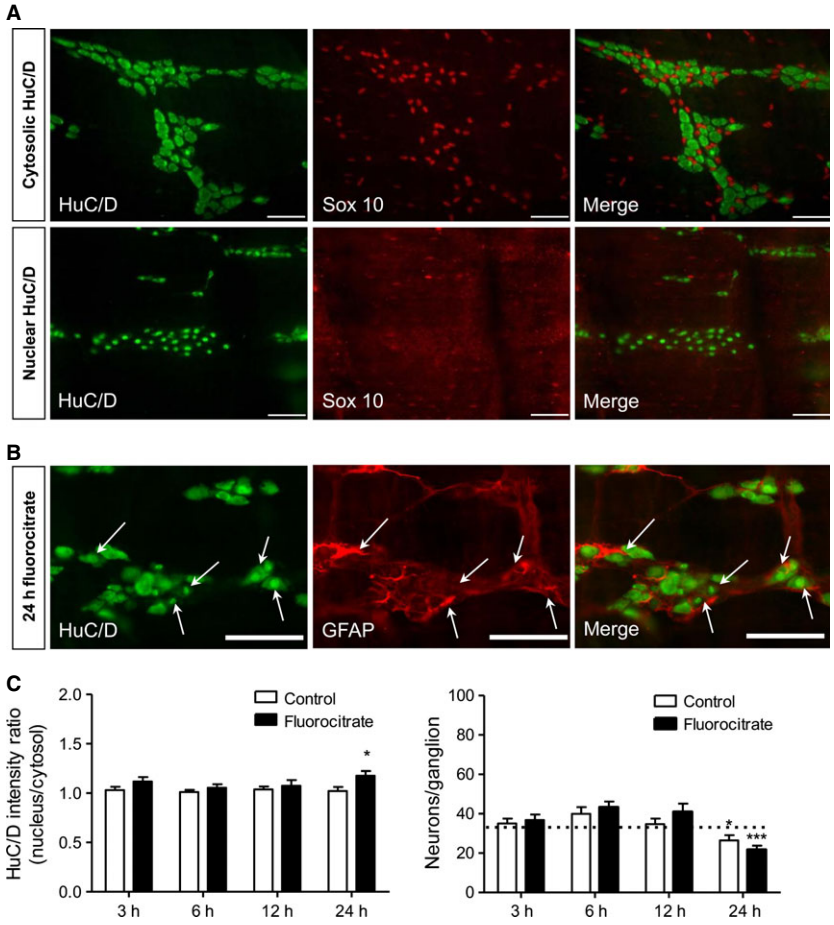

Figure 6 Enteric glial network distortion parallels the changes in HuC/D expression. (A) Representative immunohistochemical staining of neuronal marker HuC/D (*left*) and glial marker Sox10 (*middle*) in control conditions (*up*) and with nuclear localization of HuC/D (*bottom*). Note that when HuC/D staining is more intense in the nucleus of myenteric neurons, Sox10 immunoreactivity is not detectable. Merged image in A, *right*; scale bars: 100 μm. (B) Representative immunohistochemical staining of the neuronal marker HuC/D (*left*) and the glial marker GFAP (*middle*) after incubation for 24 h with gliotoxin fluorocitrate. Note the signs of GFAP overexpression (reminiscent of reactive gliosis; arrows, *middle*) and nuclear occurrence of HuC/D in neurons in the vicinity (arrows, *left*). Merged images in B, *right*; scale bars: 100 μm. (C) Graphs showing the effect of fluorocitrate incubation over time on the mean HuC/D intensity ratio nucleus/cytosol (fluorocitrate 24 h *vs* ctrl 24 h; $^{*}p < 0.05$, *left*) and the total number of HuC/D-positive neurons/ganglion (*right*; ctrl 24 h *vs* direct; $^{*}p < 0.05$, fluorocitrate 24 h *vs* direct; $^{***}p < 0.001$). The dashed line shows the average number of neurons in a directly fixed tissue (34.5 ± 2.4).

which again suggests that enteric glial cells are affected by the same type of interventions that cause nuclear HuC/D expression.

Fluorocitrate results in a dominant nuclear HuC/D immunoreactivity. To further investigate whether enteric glial cells play an active role in the localization of HuC/D, we used fluorocitrate (10 μM), a toxin reported to interfere with enteric glial metabolism.[35,36] Although not different for shorter incubations, we measured a significant increase in HuC/D intensity ratio after 24-h fluorocitrate incubation (ctrl: 1.02 ± 0.04 *vs* fluorocitrate: 1.17 ± 0.04; $^{*}p < 0.05$; Fig. 6C, left). We also found that fluorocitrate worsened the loss of HuC/D-positive neurons after 24-h incubation compared to tissues that were directly fixed (direct: 34.5 ± 2.4 *vs* control 24 h: 26.4 ± 2.7; $^{*}p < 0.05$, direct *vs* fluorocitrate 24 h: 21.7 ± 2.0; $^{***}p < 0.001$; Fig. 6C, right). Contrary to the other toxin conditions, where we found distortion of the enteric glial network (fragmentation of the GFAP pattern), fluorocitrate enhanced the GFAP expression making it reminiscent of reactive gliosis (Fig. 6B).

Nuclear HuC/D immunoreactivity is associated with a non-apoptotic genetic program

As it is not entirely clear why HuC/D is more predominant in the nucleus, we tested whether this event coincided with the activation of gene transcription. We used an antibody against the early gene product c-Fos and found a clear increase in neurons with nuclear HuC/D, while neurons with mainly cytosolic expression did not show c-Fos labeling (Fig. 7A, top). We also found that extreme and harsh damage (5% Triton X-100) to the tissue resulted in a bright nuclear HuC/D together with a positive c-Fos staining in all neurons (Fig. 7A, bottom). We also used TUNEL staining to assess the involvement of apoptotic pathways, but as shown in Fig. 7B, none of the neurons with nuclear HuC/D staining displayed signs of apoptosis.

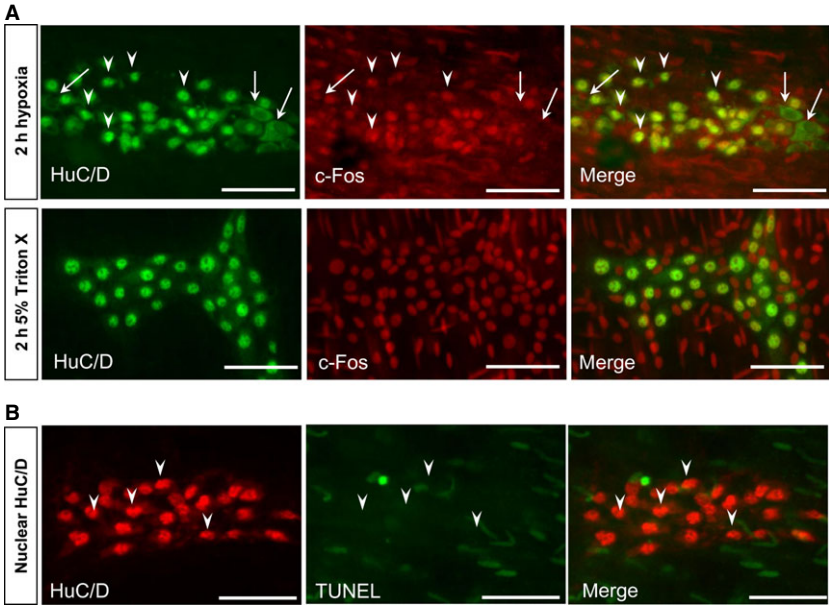

Figure 7 Nuclear localization of HuC/D coincides with the initiation of a non-apoptotic genetic program. (A, *top row*) Representative immunohistochemical staining of the neuronal marker HuC/D (*right*) in combination with the early gene c-Fos as marker for neuronal activity (*middle*) in a tissue kept 2 h in hypoxic conditions. Merged image in A, *right*. Arrows indicate neurons that display cytosolic staining for HuC/D, and have negative c-Fos nuclei. Nuclear HuC/D-stained neurons and c-Fos-positive neurons are marked by an arrowhead; scale bars: 100 μm. (A, *bottom row*) Representative image of the myenteric plexus incubated for 2 h in Krebs containing 5% Triton X-100. Note the intense nuclear HuC/D staining (*left*) in combination with a positive c-Fos staining (*middle*). Merged image in B, *right*; scale bars: 100 μm. Note that this exemplifies the most extreme case of nuclear HuC/D. (B) TUNEL staining of a representative myenteric ganglion in tissue that was mechanically damaged (scratch). HuC/D is mainly present in the nucleus (*left, arrowheads*), while no signs of apoptosis (TUNEL) can be detected (*middle, arrowheads*). Note that some muscle cells have TUNEL-positive nuclei. Merged image in B, *right*; scale bars: 100 μm.

Permeability of the nuclear envelope is not involved in HuC/D localization change

To investigate whether damage to the nuclear envelope, which at the time of immunostaining would allow antibodies to penetrate more easily into the nucleus, could explain enhanced nuclear HuC/D labeling, we performed immunostainings in high concentrations of Triton X-100 (5%) assuring full envelope permeabilization. We found no evidence for brighter nuclear staining (Fig. 8) in directly fixed tissues, which prove that antibody penetration into the nucleus is not an issue.

DISCUSSION

The use of adequate neuronal markers is crucial for the identification and characterization of neurons both in the central and in the peripheral nervous system. The specific pan-neuronal protein HuC/D is commonly used, as it allows correct quantification of neuronal cell bodies[1–3] mainly because the HuC/D antibody does not label neuronal processes. However, the widespread use of HuC/D has also revealed a remarkable heterogeneity in expression levels and subcellular localization of the protein, especially with respect to cytosolic or nuclear appearance. This

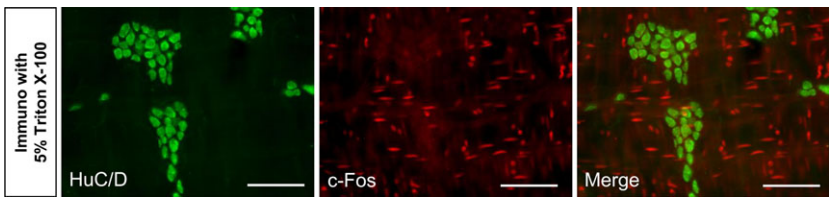

Figure 8 Permeability of the nuclear envelope is not involved in HuC/D localization change. Representative images of an immunohistochemical staining performed with blocking medium containing 5% Triton X-100 on a directly fixed myenteric plexus preparation. The HuC/D protein is present in the cytosol (*left*) and no typical nuclear staining is revealed. Note that as in other control tissues that were fixed directly, there were hardly any c-Fos-labeled (*middle*) neurons. Merged image in 8, *right*; scale bars: 100 μm.

heterogenic expression pattern, present both in central and peripheral neurons, remains poorly understood. It has been used as a read-out for enteric damage but without addressing the underlying mechanism.[22] Therefore, we decided, using *in vitro* experiments, to identify the (pathological) conditions that induce changes in HuC/D localization in enteric neurons.

Firstly, we show that time-controlled incubation in simple Krebs buffer induced changes in HuC/D expression patterns in myenteric neurons. With time, progressively more neurons with nuclear HuC/D labeling were found, which deviates from the cytosolic expression under physiological conditions (as per fixation at time 0). These data demonstrate that it is crucial to carefully consider time before fixation as an important parameter during experimental treatment of nerve tissues. Our findings also indicate that stressful environmental conditions affect both neurons and enteric glial cells, which results in translocation of HuC/D to the neuronal nucleus, while GFAP expression in enteric glial cells becomes distorted. The nuclear localization of HuC/D coincides with the activation of early gene (c-Fos), but is not necessarily linked to apoptotic signaling pathways. On the basis of these findings, we hypothesize that the altered HuC/D localization, is likely due to an active translocation of HuC/D to the nucleus, which is necessary to switch on recovery programs to deal with specific nerve-damaging conditions.

Several studies have highlighted the fact that mechanical damage can have serious consequences for tissue survival and functioning.[37] We found that mechanical damage indeed changed HuC/D expression toward a dominant nuclear localization, at least in those ganglia relatively close to the insult. In an attempt to induce more widespread damage, we applied the cationic surfactant BACl, known to destroy enteric neurons.[23,24] However, BACl incubation did not induce any difference in HuC/D expression, which indicates that the nuclear immunoreactivity is possibly specific to a certain type of damage. On the other hand, it is possible that the effect of BACl was not fully developed as it has been shown to require a full immunological activation which is not present *in vitro*.[38,39]

We further designed *in vitro* experiments using different molecules known to induce cellular or tissue stress. Neither ER stress, induced by thapsigargin, nor pro-inflammatory stimuli (TNF-α and IL-1β), resulted in more HuC/D immunoreactivity in the nucleus. Conversely, rotenone, a drug that blocks the respiratory chain by inhibiting mitochondrial complex 1, induced a significant increase in the nuclear expression of HuC/D intensity ratio after 3–6 h of incubation. Intriguingly, we did not find any significant difference after longer incubation. At the moment, it remains unclear whether a compensatory mechanism is activated or whether some neurons recover from the insult even in the presence of the toxin. These results indicate that interfering with the electron transport chain in mitochondria can alter HuC/D expression, which led us to test the effect of O_2 availability and hypoxia.

A vast amount of literature exists to show that intestinal ischemia is a significant clinical problem that leads to structural and functional changes in enteric neurons and glial cells. A hypoxic situation due to interruption of the blood supply can cause impairment of absorption, motility and intestinal barrier function.[40–42] When hypoxia was mimicked *in vitro*, we found that HuC/D had indeed accumulated in the neuronal nucleus. This change in localization was specifically due to shortage of O_2, as modification of pH did not cause any significant change. Our hypoxia experiments confirm the observations from *in vivo* ischemia/reperfusion assays, which resulted in bright nuclear HuC/D expression in over 35% of enteric neurons.[21,22] Together with the results of the rotenone incubation experiments, these data demonstrate that lack of respiration is a trigger for the change in subcellular HuC/D localization.

Throughout this study, we observed that nuclear localization of HuC/D was associated with a distortion of the GFAP expression and even a loss of Sox10 immunoreactivity in enteric glial cells. We, therefore, tested the effect of glial toxin fluorocitrate, but found only minimal effects on the localization of HuC/D. Although it is not entirely clear how enteric glial dysfunction links to nuclear HuC/D localization, the lack of effect observed here may well be due to differences in how enteric glial cells are affected by the specific toxins. Unlike the other experimental conditions in which the GFAP labeling appeared distorted, fluorocitrate treatment induced an increase in GFAP expression, reminiscent of reactive gliosis.[43] It has been shown that changes in the enteric glial network, such as distortion of GFAP expression and S100 overexpression, may occur in pathological states.[21,44,45] Experimental ablation of enteric glial cells turned out to be devastating for enteric neurons, causing severe motility disturbances, intestinal inflammation and death.[46,47] Earlier studies identified GFAP as an important component of the cytoskeleton that maintains the shape of the enteric glial cells and

allows cell branches to mechanically and functionally support neurons.[48] Phosphorylation of the N-terminal sites in these GFAP filaments results in disintegration of the processes, as shown in intestinal ischemia, which in turn can impair correct support for neurons.[21,44,49] We also observed the same GFAP characteristics when HuC/D staining became predominantly nuclear, which could indicate that due to GFAP disintegration, glial cells in the gut lose their supportive role for neurons.

The change in subcellular localization of HuC/D described in this study could be of great interest as a marker of specific damage to neurons. The functional meaning of this change in localization needs further attention and to fully comprehend the molecular consequences follow-up experiments are needed. One of the proposed hypotheses is that loss of cytosolic localization of Hu proteins contributes to mRNA degradation in the pathophysiological condition as the neuron goes into apoptosis, however our TUNEL staining argues against the involvement of apoptotic pathways. Another possibility is that the observation of nuclear HuC/D is rather technical. A degraded nuclear envelope could provide increased access for antibodies to label nuclear HuC/D only in the noxious condition. Here again, a set of experiments using high concentrations of Triton X-100 argues against this option. Another explanation is that cytosolic HuC/D proteins are degraded preferentially, while nuclear HuC/D is more protected. A last and plausible hypothesis is that Hu proteins translocate to the nucleus to interact with transcription and at the same time cease their cytosolic tasks leading to changes in translation of specific target mRNA.[14,15] Indeed, we could show that the nuclear localization of HuC/D coincides with the activation of a genetic program as the early gene c-Fos was significantly upregulated.

CONCLUSION

In conclusion, our findings support the valuable hypothesis that HuC/D is not just a pan-neuronal marker but that its cellular localization reflects the health status of neurons. In conditions of O_2 deprivation, inhibition of the mitochondrial respiratory chain, and mechanical damage, HuC/D is predominantly present in the nucleus. Additional studies in animal models are warranted to understand the molecular consequences of the change in HuC/D localization in enteric neurons.

ACKNOWLEDGMENTS

We thank the members of LENS for their critical advice and excellent technical assistance.

FUNDING

CC is post-doctoral fellow FWO. This work was funded by grants from FWO (G.0A44.13; G0889.11) and GOA (BOF, KU Leuven) to PVB.

DISCLOSURE

The authors have no financial or other conflicts to disclose.

REFERENCES

1 Phillips RJ, Hargrave SL, Rhodes BS, Zopf DA, Powley TL. Quantification of neurons in the myenteric plexus: an evaluation of putative pan-neuronal markers. *J Neurosci Methods* 2004; **133**: 99–107.
2 Freytag C, Seeger J, Siegemund T, Grosche J, Grosche A, Freeman DE, Schusser GF, Hartig W. Immunohistochemical characterization and quantitative analysis of neurons in the myenteric plexus of the equine intestine. *Brain Res* 2008; **1244**: 53–64.
3 Lin Z, Gao N, Hu HZ, Liu S, Gao C, Kim G, Ren J, Xia Y *et al.* Immunoreactivity of Hu proteins facilitates identification of myenteric neurones in guinea-pig small intestine. *Neurogastroenterol Motil* 2002; **14**: 197–204.
4 Good PJ. A conserved family of elav-like genes in vertebrates. *Proc Natl Acad Sci USA* 1995; **92**: 4557–61.
5 De Giorgio R, Bovara M, Barbara G, Canossa M, Sarnelli G, De Ponti F, Stanghellini V, Tonini M *et al.* Anti-HuD-induced neuronal apoptosis underlying paraneoplastic gut dysmotility. *Gastroenterology* 2003; **125**: 70–9.
6 Kashyap P, Farrugia G. Enteric autoantibodies and gut motility disorders. *Gastroenterol Clin North Am* 2008; **37**: 397–410, vi-vii.
7 Lennon VA, Sas DF, Busk MF, Scheithauer B, Malagelada JR, Camilleri M, Miller LJ. Enteric neuronal autoantibodies in pseudoobstruction with small-cell lung carcinoma. *Gastroenterology* 1991; **100**: 137–42.
8 Antic D, Keene JD. Embryonic lethal abnormal visual RNA-binding proteins involved in growth, differentiation, and posttranscriptional gene expression. *Am J Hum Genet* 1997; **61**: 273–8.
9 Perrone-Bizzozero N, Bird CW. Role of HuD in nervous system function and pathology. *Front Biosci* 2013; **5**: 554–63.
10 Hinman MN, Lou H. Diverse molecular functions of Hu proteins. *Cell Mol Life Sci* 2008; **65**: 3168–81.
11 Anderson KD, Sengupta J, Morin M, Neve RL, Valenzuela CF, Perrone-Bizzozero NI. Overexpression of HuD accelerates neurite outgrowth and increases GAP-43 mRNA expression in cortical neurons and retinoic

acid-induced embryonic stem cells in vitro. *Exp Neurol* 2001; **168**: 250–8.
12 Mobarak CD, Anderson KD, Morin M, Beckel-Mitchener A, Rogers SL, Furneaux H, King P, Perrone-Bizzozero NI. The RNA-binding protein HuD is required for GAP-43 mRNA stability, GAP-43 gene expression, and PKC-dependent neurite outgrowth in PC12 cells. *Mol Biol Cell* 2000; **11**: 3191–203.
13 Lim CS, Alkon DL. Protein kinase C stimulates HuD-mediated mRNA stability and protein expression of neurotrophic factors and enhances dendritic maturation of hippocampal neurons in culture. *Hippocampus* 2012; **22**: 2303–19.
14 King PH. RNA-binding analyses of HuC and HuD with the VEGF and c-myc 3′-untranslated regions using a novel ELISA-based assay. *Nucleic Acids Res* 2000; **28**: E20.
15 Deschenes-Furry J, Belanger G, Perrone-Bizzozero N, Jasmin BJ. Post-transcriptional regulation of acetylcholinesterase mRNAs in nerve growth factor-treated PC12 cells by the RNA-binding protein HuD. *J Biol Chem* 2003; **278**: 5710–7.
16 Allen M, Bird C, Feng W, Liu G, Li W, Perrone-Bizzozero NI, Feng Y. HuD promotes BDNF expression in brain neurons via selective stabilization of the BDNF long 3′UTR mRNA. *PLoS ONE* 2013; **8**: e55718.
17 Saito K, Fujiwara T, Katahira J, Inoue K, Sakamoto H. TAP/NXF1, the primary mRNA export receptor, specifically interacts with a neuronal RNA-binding protein HuD. *Biochem Biophys Res Commun* 2004; **321**: 291–7.
18 Cirillo C, Tack J, Vanden Berghe P. Nerve activity recordings in routine human intestinal biopsies. *Gut* 2013; **62**: 227–35.
19 Voss U, Sand E, Olde B, Ekblad E. Enteric neuropathy can be induced by high fat diet in vivo and palmitic Acid exposure in vitro. *PLoS ONE* 2013; **8**: e81413.
20 Phillips RJ, Kieffer EJ, Powley TL. Loss of glia and neurons in the myenteric plexus of the aged Fischer 344 rat. *Anat Embryol* 2004; **209**: 19–30.
21 Thacker M, Rivera LR, Cho HJ, Furness JB. The relationship between glial distortion and neuronal changes following intestinal ischemia and reperfusion. *Neurogastroenterol Motil* 2011; **23**: e500–9.
22 Rivera LR, Thacker M, Pontell L, Cho HJ, Furness JB. Deleterious effects of intestinal ischemia/reperfusion injury in the mouse enteric nervous system are associated with protein nitrosylation. *Cell Tissue Res* 2011; **344**: 111–23.
23 Pan WK, Zheng BJ, Gao Y, Qin H, Liu Y. Transplantation of neonatal gut neural crest progenitors reconstructs ganglionic function in benzalkonium chloride-treated homogenic rat colon. *J Surg Res* 2011; **167**: e221–30.
24 See NA, Epstein ML, Schultz E, Pienkowski TP, Bass P. Hyperplasia of jejunal smooth muscle in the myenterically denervated rat. *Cell Tissue Res* 1988; **253**: 609–17.
25 Swiercz R, Halatek T, Stetkiewicz J, Wasowicz W, Kur B, Grzelinska Z, Majcherek W. Toxic effect in the lungs of rats after inhalation exposure to benzalkonium chloride. *Int J Occup Med Environ Health* 2013; **26**: 647–56.
26 Inesi G, Hua S, Xu C, Ma H, Seth M, Prasad AM, Sumbilla C. Studies of Ca2+ ATPase (SERCA) inhibition. *J Bioenerg Biomembr* 2005; **37**: 365–8.
27 Michelangeli F, East JM. A diversity of SERCA Ca2+ pump inhibitors. *Biochem Soc Trans* 2011; **39**: 789–97.
28 Gougeon PY, Lourenssen S, Han TY, Nair DG, Ropeleski MJ, Blennerhassett MG. The pro-inflammatory cytokines IL-1beta and TNFalpha are neurotrophic for enteric neurons. *J Neurosci* 2013; **33**: 3339–51.
29 Pan-Montojo F, Schwarz M, Winkler C, Arnhold M, O'Sullivan GA, Pal A, Said J, Marsico G *et al.* Environmental toxins trigger PD-like progression via increased alpha-synuclein release from enteric neurons in mice. *Sci Rep* 2012; **2**: 898.
30 Tanner CM, Kamel F, Ross GW, Hoppin JA, Goldman SM, Korell M, Marras C, Bhudhikanok GS *et al.* Rotenone, paraquat, and Parkinson's disease. *Environ Health Perspect* 2011; **119**: 866–72.
31 Corbett AD, Lees GM. Depressant effects of hypoxia and hypoglycaemia on neuro-effector transmission of guinea-pig intestine studied in vitro with a pharmacological model. *Br J Pharmacol* 1997; **120**: 107–15.
32 Mizhorkova Z, Batova M, Milusheva EA. Participation of endogenous nitric oxide in the effect of hypoxia in vitro on neuro-effector transmission in guinea-pig ileum. *Brain Res Bull* 2001; **55**: 453–8.
33 De Giorgio R, Giancola F, Boschetti E, Abdo H, Lardeux B, Neunlist M. Enteric glia and neuroprotection: basic and clinical aspects. *Am J Physiol Gastrointest Liver Physiol* 2012; **303**: G887–93.
34 Gulbransen BD, Sharkey KA. Novel functional roles for enteric glia in the gastrointestinal tract. *Nat Rev Gastroenterol Hepatol* 2012; **9**: 625–32.
35 Fonnum F, Johnsen A, Hassel B. Use of fluorocitrate and fluoroacetate in the study of brain metabolism. *Glia* 1997; **21**: 106–13.
36 Nasser Y, Fernandez E, Keenan CM, Ho W, Oland LD, Tibbles LA, Schemann M, MacNaughton WK *et al.* Role of enteric glia in intestinal physiology: effects of the gliotoxin fluorocitrate on motor and secretory function. *Am J Physiol Gastrointest Liver Physiol* 2006; **291**: G912–27.
37 Zhou Y, Yang J, Watkins DJ, Boomer LA, Matthews MA, Su Y, Besner GE. Enteric nervous system abnormalities are present in human necrotizing enterocolitis: potential neurotransplantation therapy. *Stem Cell Res Ther* 2013; **4**: 157.
38 Parr EJ, Sharkey KA. Multiple mechanisms contribute to myenteric plexus ablation induced by benzalkonium chloride in the guinea-pig ileum. *Cell Tissue Res* 1997; **289**: 253–64.
39 Hanani M, Ledder O, Yutkin V, Abu-Dalu R, Huang TY, Hartig W, Vannucchi MG, Faussone-Pellegrini MS. Regeneration of myenteric plexus in the mouse colon after experimental denervation with benzalkonium chloride. *J Comp Neurol* 2003; **462**: 315–27.
40 Massberg S, Messmer K. The nature of ischemia/reperfusion injury. *Transpl Proc* 1998; **30**: 4217–23.
41 Alican I, Yegen C, Olcay A, Kurtel H, Yegen B. Ischemia-reperfusion-induced delay in intestinal transit. Role of endothelins. *Digestion* 1998; **59**: 343–8.
42 Udassin R, Eimerl D, Schiffman J, Haskel Y. Postischemic intestinal motility in rat is inversely correlated to length of ischemia. An in vivo animal model. *Dig Dis Sci* 1995; **40**: 1035–8.
43 Sofroniew MV. Molecular dissection of reactive astrogliosis and glial scar formation. *Trends Neurosci* 2009; **32**: 638–47.
44 Lawson VA, Furness JB, Klemm HM, Pontell L, Chan E, Hill AF, Chiocch-

etti R. The brain to gut pathway: a possible route of prion transmission. *Gut* 2010; **59**: 1643–51.
45 Ferri GL, Probert L, Cocchia D, Michetti F, Marangos PJ, Polak JM. Evidence for the presence of S-100 protein in the glial component of the human enteric nervous system. *Nature* 1982; **297**: 409–10.
46 Bush TG, Savidge TC, Freeman TC, Cox HJ, Campbell EA, Mucke L, Johnson MH, Sofroniew MV. Fulminant jejuno-ileitis following ablation of enteric glia in adult transgenic mice. *Cell* 1998; **93**: 189–201.
47 Aube AC, Cabarrocas J, Bauer J, Philippe D, Aubert P, Doulay F, Liblau R, Galmiche JP *et al.* Changes in enteric neurone phenotype and intestinal functions in a transgenic mouse model of enteric glia disruption. *Gut* 2006; **55**: 630–7.
48 Jessen KR, Mirsky R. Glial cells in the enteric nervous system contain glial fibrillary acidic protein. *Nature* 1980; **286**: 736–7.
49 Rodnight R, Goncalves CA, Wofchuk ST, Leal R. Control of the phosphorylation of the astrocyte marker glial fibrillary acidic protein (GFAP) in the immature rat hippocampus by glutamate and calcium ions: possible key factor in astrocytic plasticity. *Braz J Med Biol Res* 1997; **30**: 325–38.